The N2D Haptic Glove: A Multi-Finger Glove for 2D Directional Force Feedback for Contact Rich Manipulation

Kaitlin Calimbahin[†,1], Jake Honma[†,2], Yao-Ting Huang[†,1], Logan Li[†,3], Omar Hernandez[1], Michael C. Yip[1], *Senior Member, IEEE*

***Abstract*— Humans rely on directional fingertip cues, particularly normal forces, to probe and regulate contact during manipulation, yet most wearable gloves render only vibration or single-axis force, leaving direction ambiguous. Without directional cues, users must infer contact force from vision alone, which leads to over-pressing, inconsistent control, and reduced precision in robotic teleoperation. We present the N2D Haptic Glove, a multi-finger wearable device that renders planar vector forces at each fingertip using a compact, transparency-focused mechanical design with on-hand actuation that preserves natural motion. Through benchtop validations and teleoperation user studies involving haptically teleoperating a humanoid robot, we demonstrate that multi-directional fingertip feedback significantly improves user ability to regulate contact, reduce overshoot, and improve consistency in interactions compared to visual-only or 1D haptic feedback. These findings establish the N2D Haptic Glove and directional finger-based haptics device as an important modality for contact-rich teleoperation, immersive simulation, and robot learning from demonstrations.**

I. Introduction

Haptic devices have been utilized in various immersive contexts, ranging from interacting with virtual reality (VR) environments in simulation to teleoperating robots for minimally invasive surgery [1]. Moreover, recent interest in using human demonstrations to train robots involves human teleoperators controlling manipulators within real or virtual worlds, where haptic feedback has been shown to collect tighter and more informed distributions of trajectories for robot learning [2].

Most current haptic devices primarily provide proprioceptive feedback to the hand, with most interfaces involving the user hand grasping a handle [3] or stylus [4]. Other forms of haptic feedback exist that involve vibrotactile sensations, but do not provide the necessary kinesthetic feedback for force rendering [5].

One exciting area with limited exploration is multi-fingered haptic feedback. Providing force feedback independently to each finger can be especially beneficial for the operation of humanoid robots with multiple fingers, which is rapidly increasing in popularity for research and industry [6]. However, while a variety of methods currently exist to provide haptic feedback to fingers, from tendon-driven gloves [7] to finger-mounted vibration pads [8], an important limitation remains - the lack of comprehensive fingertip haptics capable of reproducing both normal and tangential forces.

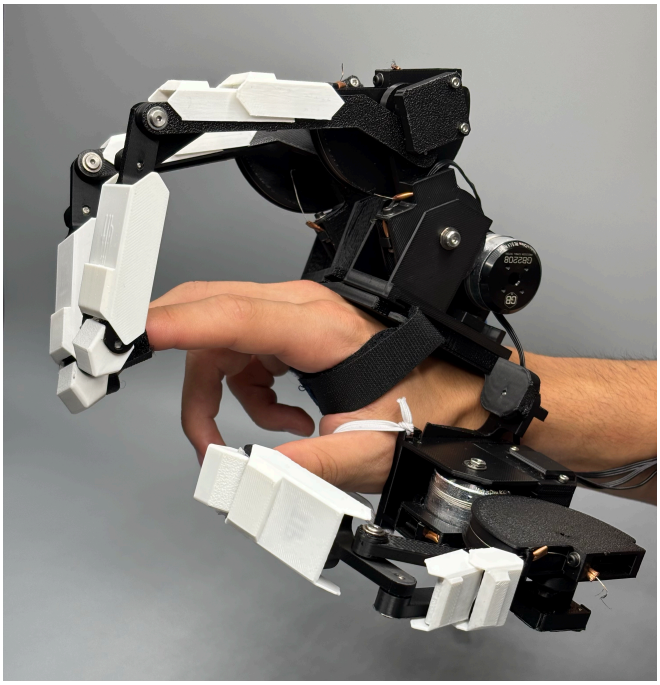

Fig. 1: **The N2D Haptic Glove:** is the first, multi-fingered glove design that offers directional force feedback on each finger. The glove provides directional haptic rendering, an integral feedback capability for contact-rich VR and robot telestration, e.g, probing, object slipping, etc., all which rely on directional forces to be rendered to the operator.

Directional haptic rendering in finger interactions remains largely underdeveloped. Consider moving a finger through a cluttered set of objects: the perception of axial forces at the fingertip can be just as vital — if not more so — than the sensation of transverse forces produced along the closing direction of the fingers. Measurements such as slip and axial probing force cannot be provided to the fingers without rendering directional force. One indirect approach is to use skin-shear on a held device [9], [10]; however, a more direct approach to providing directional force feedback to *individual fingers* is considerably more natural and interpretable.

In this paper, we present the first wearable haptic interface

† Equal contribution.

[1] Electrical and Computer Engineering, University of California San Diego, La Jolla, CA 92093, USA.

[2] Mechanical and Aerospace Engineering, University of California San Diego, La Jolla, CA 92093, USA.

[3] Bioengineering, University of California San Diego, La Jolla, CA 92093, USA.

capable of rendering multi-axial fingertip forces, including axial forces for probing and opposing normal forces for pinching and contact resistance, across multiple fingers. Named the N2D Haptic Glove — for *N* fingers and 2D force rendering per finger — the system provides a substantial increase in the dimensionality of haptic feedback for contact-rich manipulation, with potential applications in VR simulations, robot teleoperation, and imitation learning pipelines with physics-based simulators or real robots.

The key novel contributions of this paper are as follows:

1) The first multi-fingered haptic glove capable of delivering multi-axial forces to the fingertips,
2) Design and modeling of the N2D Haptic Glove interface that supports highly transparent, frictionless transmissions and clean haptic rendering. These qualities are essential for multi-degree-of-freedom (DOF) haptic interfaces that invoke effortless articulation,
3) Validation of directional feedback ability on benchtop testing, and
4) a user study demonstrating the benefits of N2D Haptic Glove's enhanced directional haptics in a humanoid robot user study.

II. Related Works

In the realm of fingertip haptics, existing wearable interfaces can be grouped by the type of force modality they primarily support: normal forces, shear and slip forces, resistive or antagonistic tendon forces.

Several methods attempt to provide direct normal forces at the fingerpads. Vibrotactile actuators, such as small fingertip-mounted vibration pads, can simulate contact events and enhance palpation cues [11], [12], while pneumatic actuators apply localized pressure through inflatable chambers and soft pressurized structures [13], [14], [15], [16]. Electromechanical methods such as electromagnetic brakes and clutches similarly provide resistive force cues during contact [17], [18]. However, vibrotactile cues stimulate only the skin and fail to deliver sustained contact forces, while pneumatic and electromechanical methods tend to be bulky, difficult to miniaturize, or limited in force output, restricting portability and multi-finger integration.

Other devices target tangential or shear forces to simulate slip or lateral motion at the fingertip. Microvibration sensing has been applied to convey texture and slip-related cues [19], while skin-stretch devices use multi-directional deformation to generate tangential cues [8], approximate weight or grasping sensations [20], or substitute missing tactile information with multi-DOF cutaneous cues [21], [22]. These designs can reproduce important slip-related interactions but are often bulky or confined to cutaneous feedback rather than true kinesthetic rendering, limiting their fidelity for dynamic manipulation tasks.

Another class of gloves emphasizes resistive forces between opposing digits, enabling pinch-like interactions. Tendon and cable-driven systems route antagonistic cables through glove structures to deliver resistive kinesthetic feedback [23], [24], while some designs combine cable actuation with vibrotactile stimulation to support hybrid cutaneous and kinesthetic sensations [25]. These systems run tendons through channels that experience friction, tendencies for curve realignment causing finger twist, and often have bulky off-hand motors or tendon-routing hardware that reduce transparency and hinder wearability.

Finally, some commercial systems exist. Dexmo offers multi-digit resistive feedback but only in flexion/extension, without probing or shear forces [26]. HaptGlove delivers untethered cutaneous and joint-level resistance but confines fingertip actuation to normal indentation [27]. Fluid Reality achieves compact wireless pressure and shape cues, yet these remain only on the finger pad [16]. AirPush demonstrates controllable shear forces but is limited to a single tethered finger device [28]. Collectively, these systems mark progress, but none combine probing, shear, and opposition forces in an untethered, multi-digit glove. The N2D Haptic Glove (non-commercial) is able to satisfy these requirements (Table I).

III. Methods

The following sections will be described in the following order: (A) A mechanical design overview of the N2D Haptic Glove, (B) discussion of the electromechanical framework, (C) a detailed description of the compact linkage design for achieving directional force per finger, (D) the kinematic analysis of the glove, and (E) a directional haptic rendering approach for multi-fingered force reflectance.

A. Mechanical Design Overview

The design of the haptic glove is based on the biomechanical degrees of freedom of the human hand. Following established biomechanical models, hand movement is often simplified to planar motions of flexion and extension, which occur at the metacarpophalangeal (MCP), interphalangeal (PIP), and distal interphalangeal (DIP) joints of the fingers, together with adduction and abduction, which describe the lateral spreading and closing of the fingers relative to the middle of the hand. While most fingers primarily operate through flexion and extension planar motions, the thumb is unique in also enabling adduction and abduction at the trapeziometacarpal (TMCJ) joint – a movement essential for precision when grasping objects. Alongside the thumb and index finger, the middle finger provides additional stability and support during grasping, making these three digits central to most everyday picking up and probing tasks. This reduction to a two degrees of freedom (2DOF) model offers a practical yet physiologically accurate framework for hand kinematics, and has been validated in computational simulations of lateral pinch that replicate physiological joint behavior with high fidelity [29].

The N2D Haptic Glove comprises multiple directional haptic subsystems per finger, articulated along a structural backbone. Each finger that provides force feedback is equipped with a linkage system offering 2DOF. These linkage systems are mounted on passive rotary joints that allow adduction and abduction between fingers, while the thumb requires additional mobility and is therefore supported

TABLE I: Comparison of Fingertip-Feedback Systems

#	Feature	PHANToM Haptic	Dexmo	HaptGlove	Fluid Reality	AirPush	Ours
1	Multi-Digit (simultaneous)	✗	✓	✓	✓	✗	✓
2	Untethered / Wearable	✗	✓	✓	✓	✗	✓
3	Directional Fingertip Forces (Multi-DoF)	✓	✗	✗	✗	✓	✓

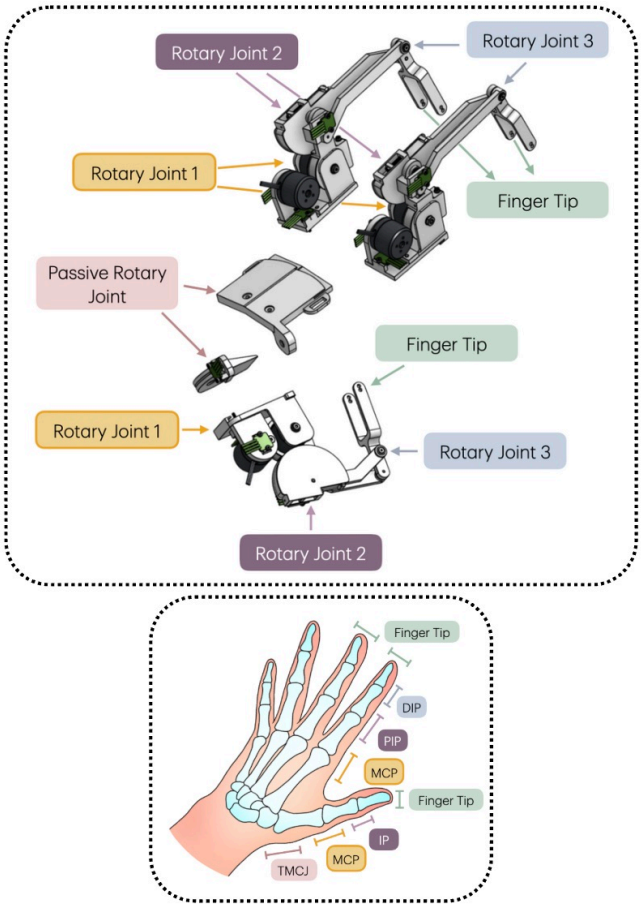

Fig. 2: **A deconstructed view of the N2D Haptic Glove.** The modular design of $N = 3$ 2D haptic linkage systems per finger, on a passive knuckle joint, provides accommodation for varying hand sizes. The 4th and 5th fingers are not provided haptic feedback in this design due to size versus motor size tradeoffs, but could reasonably be added in other variations on the N2D design.

by an extra passive rotary joint. The directional force linkage design for each finger is based on a parallel mechanism, with planar control achieved by rotating the proximal linkages through a capstan cable-drive (further detailed in the kinematic modeling section). This structure aligns with biomechanical models of the finger, where the MCP joint is treated as a saddle joint allowing flexion–extension and adduction–abduction, and the PIP and DIP joints are modeled as rotary joints constrained to flexion–extension [30] but also enables controlled directional force feedback on each finger, as illustrated in Figure 2.

In addition to enabling directional force feedback per finger, a key design feature is that haptic transparency is prioritized in the haptic glove design. Friction and damping caused by non-ideal transmissions (using gears, servomotor gearing stages, belt drives) can result in non-negligible clouding of haptic signal-to-noise-ratio (SNR), and thus negatively affect the wearer's experience – while additionally causing strain to the wearer. Thus, direct-drive ungeared motors with capstan drives are used for all active DOF. Motors are furthermore positioned such that their masses do not translate, avoiding the feeling of the inertia of a moving motor on the user's hand. In short, all mechanical considerations (cable-driven, ungeared motors, no flying motors, linkage systems over tendons and tendon routings, bearing-supported axles) were chosen for high haptic transparency for the N2D glove.

One unique characteristic of the mechatronics design of the glove is that the mechanical transmissions do not extend beyond the wrist. While the weight of carrying components can be a concern, a design choice was to keep all mechanisms to the hand and not beyond the wrist, which can provide significant resistance, strain, hysteresis, and dead zones, and unmodeled dynamics to the wearer's wrist, issues that can arise with hoses from Bowden cable drives and hydraulic or pneumatic actuation (e.g. HaptX glove, requiring a backpack). The overall weight of the N2D glove is 562 g, which is broken down in Table II.

TABLE II: Weight Breakdown of the N2D Haptic Glove

Qty	**Component**	**Unit Weight (g)**	**Total (g)**
6	Gimbal Motor	39.5	237
6	Motor Driver	4.5	27
10	Encoder	1	10
1	Main PCB	6	6
1	Teensy 4.1	8	8
—	PLA & COTS parts	274	274
		Total Weight:	**562**

B. Electromechanical Architecture

Figure 3 summarizes the electromechanical stack and distributed control that enable torque-transparent direct-drive actuation in the N2D Haptic Glove. Direct-drive GB2208 gimbal motors were chosen as they are currently the smallest, commercially available gimbal motor (high-torque output, low speed) without planetary gearing. The motors are powered by DRV8313 three-phase drivers from an 14 V rail and instrumented with AS5048B 14-bit absolute magnetic encoders for rotor angle feedback. Each motor–encoder pair interfaces with a Teensy 4.1 microcontroller executing field-oriented control (FOC) in torque mode at **10 Hz,** while

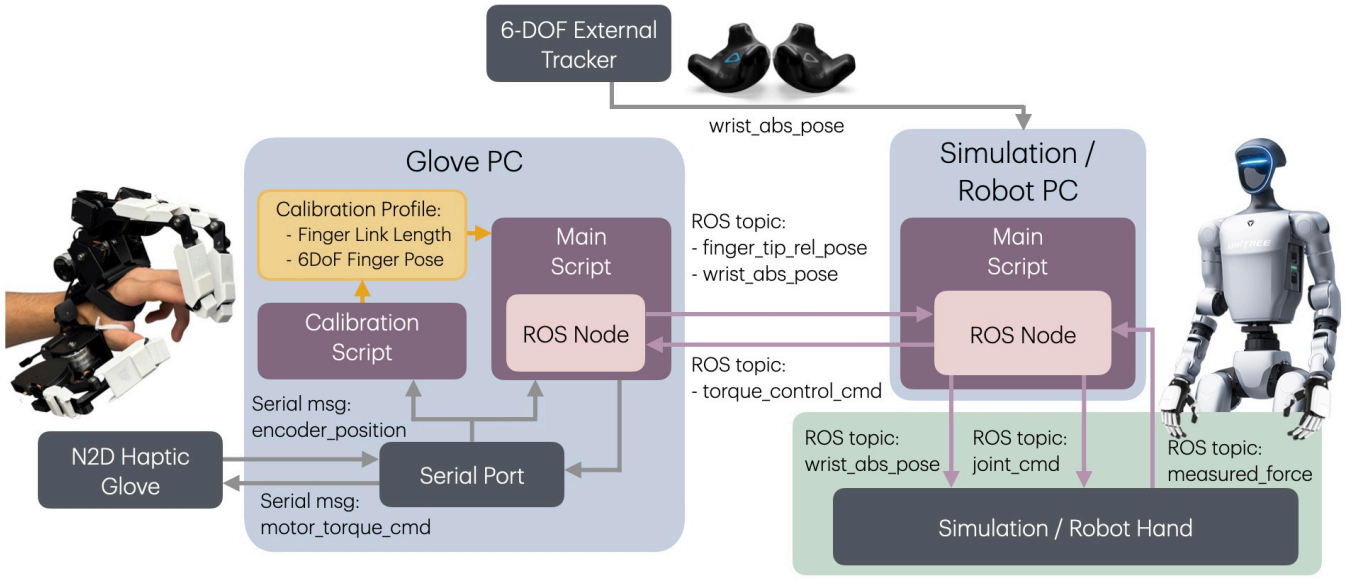

Fig. 3: Control Block Diagram Showing the System Architecture. The N joints run independent torque control, serially communicating with a common microcontroller that performs kinematic and haptic rendering mappings from Cartesian space to joint space and serially communicating with a PC. Initialization of kinematics is required for accurate directional force rendering to account for hand sizes.

higher-level computation runs on the Glove PC within a ROS-based, serial-linked architecture.

On the Glove PC, a calibration script generates a user-specific profile containing finger link lengths and 6-DOF finger poses. This profile is used by the main control script, which communicates through a ROS node. The glove hardware exchanges encoder position data and motor torque commands with the PC over a serial connection, enabling real-time torque control. A 6-DOF external tracker provides the absolute wrist pose, which is published as a ROS topic and combined with fingertip pose estimates. On the Simulation/Robot PC, a corresponding ROS node receives these poses and issues commands to either a simulated environment or a physical robot hand. The robot or simulation reports back measured forces, which are relayed through the ROS node and returned as torque control commands to the glove. This communication, covering fingertip relative pose, wrist pose, joint commands, and measured forces closes the loop between the glove and the simulated or physical hand. By distributing calibration, control, and simulation across PCs, the architecture supports scalability to multiple fingers, reduces latency, and maintains mechanical transparency.

C. Kinematic Modeling

Each kinematic model providing position and forces relative to the base joint will need to be mapped to a hand coordinate frame to measure their positions relative to the hand. Then, the hand must be measured in its position in space so as to localize each digit (and hand by implication) in the world frame in order to assign the proper haptic feedback – either by checking for contact in VR or resolving forces measured on a robotic hand. To describe the kinematics of the overall system, we will define the device as a collection of serial linkages fixed on a common base (Fig. 4), with each link being a rigid body with orientation $\mathbf{R} \in SO(3)$ and position $\mathbf{p} \in \mathbb{R}^3$. A transformation between bodies is represented by a homogeneous transform

$$\mathbf{T}_i^j = \begin{bmatrix} \mathbf{R}_i^j & \mathbf{p}_i^j \\ \mathbf{0}_{1\times 3} & 1 \end{bmatrix} \tag{1}$$

which describes tensors in coordinate frame i in a new coordinate frame j.

We define a canonical base frame for the device $\{base\}$ with fixed origin (conveniently set at the position-tracker's origin and orientation). Each digit, $f \in \{\text{T,I,M}\}$ (Thumb, Index, Middle) has a constant base coordinate frame $\mathbf{T}_{T,base}^{base}, \mathbf{T}_{I,base}^{base}, \mathbf{T}_{M,base}^{base}$ described in the position-tracker origin. For non-thumb fingers ($f = I,M$), the kinematics of the linkages from the finger's base $f,base$ to the tip can be described use three revolute joints $q_{f,0}, q_{f,1}, q_{f,2}$ and link lengths $a_{f,0}, a_{f,1}, a_{f,2}, a_{f,3}$. The distal tip pose $\{tip\}$ described in the base frame $\{base\}$ is

$$\begin{aligned} \mathbf{T}_{f,tip}^{f,base}(\mathbf{q}^f, \mathbf{a}^f, \mathbf{l}^f) = \mathbf{T}_{f,0}^{f,base}\, \mathbf{T}_{f,1}^{f,0}\, \mathbf{T}_{f,B}^{f,1}\, \mathbf{T}_{f,D}^{f,B}\, \mathbf{T}_{f,tip}^{f,D} = \\ \begin{bmatrix} \mathbf{R}_y(q_{f,0}) & \mathbf{0}_{3\times 1} \\ \mathbf{0}_{1\times 3} & 1 \end{bmatrix} \begin{bmatrix} \mathbf{R}_z(q_{f,1}) & \mathrm{tr}_x(a_{f,0}) \\ \mathbf{0}_{1\times 3} & 1 \end{bmatrix} \\ \begin{bmatrix} \mathbf{R}_z(q_{f,2}) & \mathrm{tr}_x(a_{f,1}+l_3) \\ \mathbf{0}_{1\times 3} & 1 \end{bmatrix} \begin{bmatrix} \mathbf{R}_z(q_{f,3}) & \mathrm{tr}_x(l_2) \\ \mathbf{0}_{1\times 3} & 1 \end{bmatrix} \\ \begin{bmatrix} \mathbf{I}_{3\times 3} & \mathrm{tr}_x(a_{f,3}) \\ \mathbf{0}_{1\times 3} & 1 \end{bmatrix} \end{aligned} \tag{2}$$

where $\mathbf{R}_z$ is the 3×3 rotation matrix about z and $\mathbf{tr}_x(a_{(\cdot)}) = [a_{(\cdot)}, 0, 0]^\top$. Angle $q_{f,3}$ is driven by $q_{f,1}$ and $q_{f,2}$. We solve $q_{f,3}$ via the cosine law by first computing the diagonal CD,

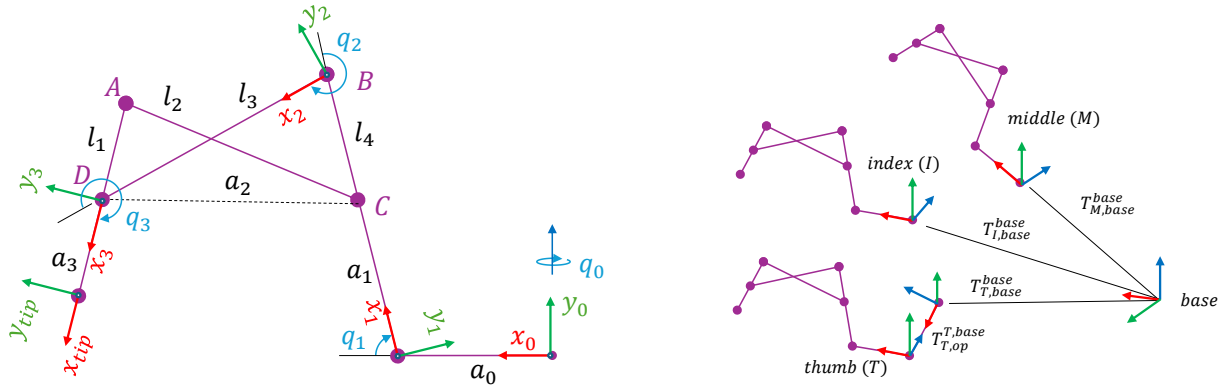

Fig. 4: Kinematic Analysis of a Finger Linkage: On the left, a single finger linkage with three DOFs defined by $0,1,2$ (with 3 being a driven joint by 1 and 2) is shown. On the right shows the layout of finger linkages on the glove body, showing the overall coordinate frames. In addition, the thumb has an extra DOF for opposition.

then the internal angles $\angle ADC$ and $\angle BDC$, and finally taking their difference. Such that

$$CD = a_{f,2} = \sqrt{l_2^2 + l_3^2 + 2l_2 l_3 \cos 2} \tag{3}$$

$$\angle ADC = \arccos\left(\frac{l_1^2 + a_{f,2}^2 - l_1^2}{2l_1 a_{f,2}}\right) \tag{4}$$

$$\angle BDC = \arccos\left(\frac{l_2^2 + a_{f,2}^2 - l_3^2}{2l_2 a_{f,2}}\right) \tag{5}$$

$$q_{f,3} = \angle ADC - \angle BDC \tag{6}$$

The resultant position of each finger in it's base frame is

$$x^{f,base}_{f,tip} = \mathrm{c}_0(a_{f,0} + l_1\mathrm{c}_{123} + l_{f,3}\mathrm{c}_{12} + (a_{f,1} + l_{f,4})\mathrm{c}_1) \tag{7}$$

$$y^{f,base}_{f,tip} = l_{f,2}\mathrm{s}_{123} + l_{f,3}\mathrm{s}_{12} + (a_{f,1} + l_{f,4})\mathrm{s}_1 \tag{8}$$

$$z^{f,base}_{f,tip} = -\mathrm{s}_0(a_{f,0} + l_{f,2}\mathrm{c}_{123} + l_{f,3}\mathrm{c}_{12} + (a_{f,1} + l_{f,4})\mathrm{c}_{f,1}) \tag{9}$$

with shorthand notation used, e.g., $\mathrm{s}_0 = \sin(q_{f,0})$ and $\mathrm{c}_{123} = \cos(q_{f,1} + q_{f,2} + q_{f,3})$.

For the thumb ($f = \mathrm{T}$), we have an additional passive joint providing affordance for opposition. Thus, the thumb has a modified transformation:

$$\mathbf{T}^{T,base}_{T,tip}(\mathbf{q}^T, \mathbf{a}^T) = \mathbf{T}^{T,base}_{T,op}\ \mathbf{T}^{T,op}_{T,0}\ \mathbf{T}^{T,0}_{T,1}\ \mathbf{T}^{T,1}_{T,B}\ \mathbf{T}^{T,B}_{T,D}\ \mathbf{T}^{T,D}_{T,tip} \tag{10}$$

where $\mathbf{T}^{T,base}_{T,op} = \begin{bmatrix} \mathbf{R}_z(q_{T,op}) & \mathbf{tr}_x(a_{T,op}) \\ \mathbf{0}_{1\times 3} & 1 \end{bmatrix}$ describes the additional link transform that is applied as a pre-multiplication to the rest of the serial transformations, and then $\mathbf{T}^{T,op}_{T,0} = \begin{bmatrix} \mathbf{R}_y(q_{f,0}) & \mathbf{0}_{3\times 1} \\ \mathbf{0}_{1\times 3} & 1 \end{bmatrix}$, resulting in the thumb tip position at

$$\begin{aligned} x^{T,base}_{T,tip} &= a_0\mathrm{c}_0\mathrm{c}_{op} + a_{op} - l_2(\mathrm{s}_{op}\mathrm{s}_{123} - \mathrm{c}_0\mathrm{c}_{op}\mathrm{c}_{123}) - l_3(\mathrm{s}_{op}\mathrm{s}_{12} \\ &\quad - \mathrm{c}_0\mathrm{c}_{op}\mathrm{c}_{12}) - (a_1 + l_4)(\mathrm{s}_1\mathrm{s}_{op} - \mathrm{c}_0\mathrm{c}_1\mathrm{c}_{op}) \end{aligned} \tag{11}$$

$$\begin{aligned} y^{T,base}_{T,tip} &= a_0\mathrm{s}_{op}\mathrm{c}_0 + l_2(\mathrm{s}_{op}\mathrm{c}_0\mathrm{c}_{123} + \mathrm{s}_{123}\mathrm{c}_{op}) + l_3(\mathrm{s}_{op}\mathrm{c}_0\mathrm{c}_{12} \\ &\quad + \mathrm{s}_{12}\mathrm{c}_{op}) + (a_1 + l_4)(\mathrm{s}_1\mathrm{c}_{op} + \mathrm{s}_{op}\mathrm{c}_0\mathrm{c}_1) \end{aligned} \tag{12}$$

$$z^{T,base}_{T,tip} = -(a_0 + l_2\mathrm{c}_{123} + l_3\mathrm{c}_{12} + (a_1 + l_4)\mathrm{c}_1)\mathrm{s}_0 \tag{13}$$

Given the pose of the glove in the world $\mathbf{T}^w_{base}$, as measured by an optical tracker, we can derive the pose (position and orientation) of each finger in the world via

$$\mathbf{T}^w_{f,tip} = \mathbf{T}^w_{base}\ \mathbf{T}^{base}_{f,base}\ \mathbf{T}^{f,base}_{f,tip} = \begin{bmatrix} \mathbf{R}^w_{f,tip} & \mathbf{p}^w_{f,tip} \\ \mathbf{0}_{1\times 3} & 1 \end{bmatrix} \tag{14}$$

The position of finger tips ($f = \{I, M\}$) in the world are thus

$$\mathbf{p}^w_{f,tip} = \begin{bmatrix} x^w_{f,tip} & y^w_{f,tip} & z^w_{f,tip} \end{bmatrix}^\top \tag{15}$$

and the resultant position of the thumb in the world is:

$$\mathbf{p}^w_{T,tip} = \begin{bmatrix} x^w_{T,tip} & y^w_{T,tip} & z^w_{T,tip} \end{bmatrix}^\top. \tag{16}$$

D. Multi-digit Haptic Rendering

Rendering directional haptics to each digit involves mapping of cartesian forces in the world, $\mathbf{f}^w_f \in \mathbb{R}^3$ to motor torques on the fingers $\tau_f \in \mathbb{R}^2$. This is done using

$$\tau_f = \mathbf{J}^w_f(\mathbf{q}_f)^\top \mathbf{f}^w_f \tag{17}$$

where $\mathbf{J}^w_f(\mathbf{q}_f) = \begin{bmatrix} \frac{\partial \mathbf{p}^w_f}{\partial q_{f,1}}, \frac{\partial \mathbf{p}^w_f}{\partial q_{f,2}} \end{bmatrix} \in \mathbb{R}^{3\times 2}$ is the Jacobian matrix of the position vector $\mathbf{p}^w_f$ with respect to the joint angles $\mathbf{q}_f$. Because of the limitations of the active 2DOF device, forces will project onto the controllable plane of the active DOF of the device, which is the plane in which the kinematic linkages of each finger spans.

Ultimately, the uncontrolled direction, related to finger adduction and abduction, is not reflected. This is due to concerns of weight and volume; there are limitations on design. While a third dimension of haptic sensation could be rendered by additional actuation at the linkage base, resulting in finger adduction and abduction, the extra 50% weight increase was a design decision to skip for this study. We will demonstrate the advantage of the 2D directional force feedback on enabling certain probing, slip, and shear tasks to be performed, and show both the advantages of moving from 1D to 2D in the experiments section.

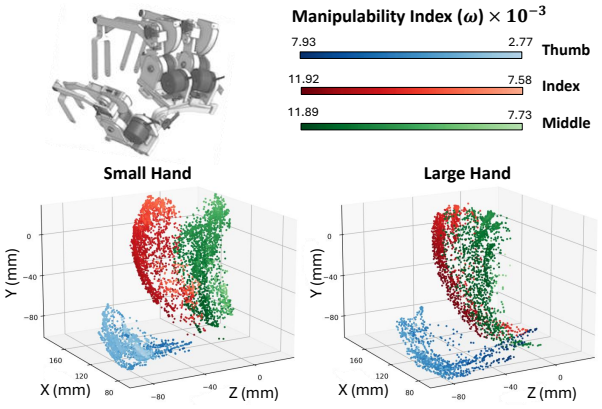

Fig. 5: Range of motion image for hands, small and large hands, showing that the N2D Haptic Glove allows for can encapsulation of nearly all ranges of motion.

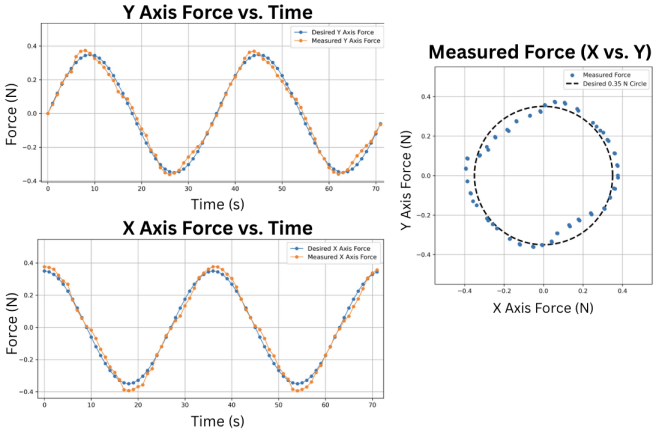

Fig. 6: Measured vs. commanded fingertip force directions. Errors in directional force rendering are low, confirming that the N2D Haptic Glove's linkage and control system generate accurate directional forces and motivating minor user-specific calibration.

IV. Experiments and Results

We conducted a series of validation experiments along with a teleoperation user study to provide both quantitative and qualitative assessments of the N2D Haptic Glove, demonstrating its performance in controlled force rendering tasks as well as its effectiveness in real-world robotic teleoperation.

A. Validation Experiments

1) Comparing Reachable Space of Human and Device: We began by examining how the N2D Haptic Glove influences users' natural range of motion, with particular attention to interphalangeal joint flexion/extension and knuckle abduction/adduction. To evaluate whether the N2D Haptic Glove introduced any restrictions, two participants representing small and large hand sizes performed maximum flexion and extension of their fingers, as well as lateral abduction and adduction at the knuckles. Hand size was measured as the straight-line distance from the distal wrist crease to the tip of the middle finger; our small and large participants measured approximately 15.4 cm and 20.5cm, which sit within adult hand-length distributions (about 15–23 cm across large U.S. adult samples) [31]. As shown in Figure 5, the N2D Haptic Glove preserved nearly the full range of motion across all tested joints between small and large hand sizes. To further evaluate the N2D Haptic Glove's capacity for rendering multi-directional forces, we computed the manipulability index across the observed joint configurations. This index,

$$w(\mathbf{q_f}) = \sqrt{\det(\mathbf{J_f^w}(\mathbf{q_f})\mathbf{J_f^w}^\top(\mathbf{q_f}))} \tag{18}$$

where $w(\mathbf{q_f}) \to 0$ approaches a singularity and results in joint locking and therefore should be avoided. The N2D Haptic Glove maintained highest manipulability throughout the majority of the workspace for fingers, with the manipulability index changing approximately 30% to 60% that

confirming that it can generate directional forces without constraining the user.

2) Planar Joint Actuation Experiment: A mapping between input voltage and output torque at the joint is found via a directional calibration method. Ideally the voltage-current relationship is perfectly linear but in practice cogging behaviors as well as material strain can produced nonlinear relationships. A 2-axis force sensing setup with two 1kg load cells is mounted in a perpendicular configuration to measure planar forces. A haptic finger linkage with its base fixed has its tip connected to the force sensor setup. Assuming low speeds, we can ignore back-EMF effects and convert voltage $\mathbf{v}_f \in [v_{f,1}, v_{f,2}]$ to each motor to torque at each joint $q_{f,1}, q_{f,2}$ via the relationship

$$\tau_f = \begin{bmatrix} \zeta_1 \cdot f_{poly}(v_{f,1}, \mathbf{k}_{f,1}) & 0 \\ 0 & \zeta_2 \cdot f_{poly}(v_{f,2}, \mathbf{k}_{f,2}) \end{bmatrix} \tag{19}$$

where ζs are the gearing ratios provided by the capstan drive and $\mathbf{k}$s are coefficients of a polynomial to be solved (the motor torque constants). Via a series of voltage sweeps, $\mathbf{v}_f$, and measured forces from the force sensor, $\mathbf{f}_f^w$, the coefficients can be solved for with Eq. 17 in closed form using a least-squares fit. Each finger is calibrated once for the optimal polynomial and coefficients.

Figure 6 shows the measured forces during testing closely matching the commanded vectors, with consistent alignment in both magnitude and direction. These results confirm that the voltage-to-torque mapping, when combined with the glove's kinematic structure, accurately produces the intended fingertip forces. Minor deviations suggest that 3D printed compliance of the glove may be causing directional accuracy to stray in certain configurations, but overall, the N2D Haptic Glove demonstrates robust and reliable force rendering. This validation not only confirms the accuracy of the voltage–torque model in practical operation but also provides confidence in the glove's ability to deliver controlled, multidirectional force feedback for subsequent VR simulation and teleoperation experiments.

3) Haptic Teleoperation with Humanoid Experiment: Pushing buttons, while seemingly trivial, presents a challenge for teleoperation scenarios without proper haptic feedback. The push task was selected because it captures a second essential manipulation primitive: probing and confirming discrete contacts. In teleoperated environments such as operating control panels or medical equipment, an accurate pushing force is critical. Vision alone cannot always confirm contact, especially when buttons have small travel distances or provide little visual motion, and 1D haptic cues may be insensitive at oblique or out-of-axis misalignments.

In our study, participants teleoperated the G1-humanoid robot (Unitree) with the RH56DFTP (Inspire Robotics) humanoid hands, with tactile array sensing, to press down on a digital scale while wearing the N2D Haptic Glove under three feedback modes: no haptics (visual feedback only), 1D haptics, and 2D haptics. Users wore the N2D glove, and were given a live video-stream for visual feedback. The experiment consisted of two modes —– axial probing (finger tip) and transverse probing (finger pad) by the robot fingers —–- each tested under all three feedback modes. Within each mode, participants completed two force-regulation tasks: making light contact with the scale, barely touching the scale (light force), and pressing with 500 g of force (heavy force). Before beginning the tasks, participants received training to calibrate their perception by pressing the scale directly with their finger to experience the target levels for light and heavy force, several times. During the study, the true scale forces were hidden from the user. Users completed a NASA-TLX [32] survey afterwards. Performance was evaluated by measuring the range of force applied on the scale against a target threshold for each task. Consistency was assessed across repeated trials, with narrower force variability indicating greater control.

Figure 7 shows the results of the user study. In both axial and transverse probing, participants in the no-haptics condition consistently overshot the target ranges, pressing harder than required due to reliance on vision alone. With 1D haptics, participants showed moderate improvement but continued to struggle with precise regulation, particularly at medium and heavy force levels. By contrast, 2D haptics produced the most accurate and stable performance, reducing overshoot and undershoot while lowering trial-to-trial variability. Subjective feedback aligned with these trends as NASA TLX ratings indicated that participants perceived lower workload, reduced frustration, and higher control and confidence with 2D haptics compared to either 1D haptics or no haptics as seen in Figure 8.

Taken together, results from our user study show that multi-directional haptic feedback enhances both objective force regulation and subjective user experience in teleoperated tasks.

V. Discussions and Conclusions

Directional haptic feedback on the fingers is critical for achieving realistic physical interaction in teleoperated systems. We presented the design, analysis, benchtop validation,

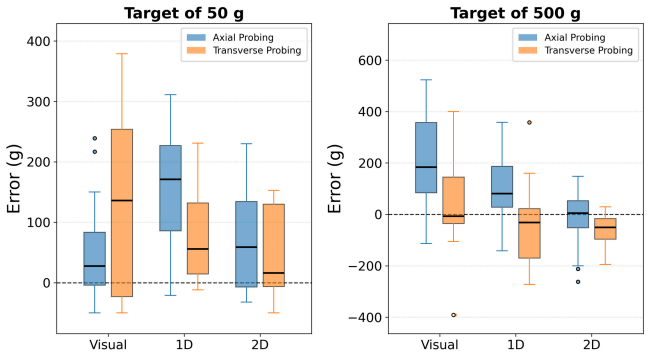

Fig. 7: Boxplots of signed error (g) for Target of 50 g and Target of 500 g. Across both Axial Probing and Transverse Probing, 1D haptic feedback is more accurate than Visual-only, and 2D haptic feedback is more accurate than both, as shown by lower median error.

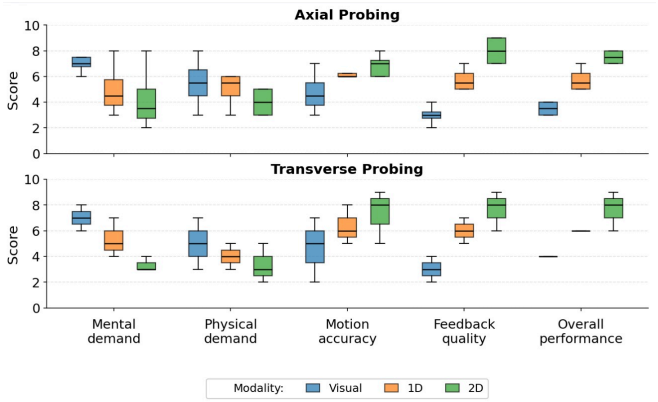

Fig. 8: NASA TLX results for the three conditions, demonstrating that the directional haptics show significant value in reduction of cognitive load and perceived interaction quality over 1D or non-haptic approaches.

and user studies of the value of directional haptics in the N2D Haptic Glove. Across controlled validation experiments and through our user study, we found that multi-directional haptics consistently improved task performance and reduced variability in applied force. These results confirm that it is not simply the presence of haptic cues, but specifically their directionality, that allows users to regulate force with accuracy, consistency, and confidence.

Designing a haptic glove requires a careful balance between force fidelity and physical comfort. Our design demonstrates that lightweight linkages and compact actuation can achieve accurate directional force rendering while still preserving the user's natural range of motion. At the same time, tradeoffs remain. The glove introduces minor deviations in force direction that motivate user-specific calibration, and the weight of the glove can make it tiring to use over time, thereby limiting its use only for haptically sensitive tasks. These limitations highlight the difficulty of creating a device that is simultaneously precise, wearable, and scalable. However, with user-specific calibrations, and improvements in gimbal motor miniaturization (GB2208 is the smallest

gimbal motor on the market today, but drone technology is pushing these products smaller at a rapid pace), these limitations shall eventually be surpassed, even offering an N3D option in the future.

In conclusion, the N2D Haptic Glove demonstrates that multi-directional haptics is not only feasible but valuable for contact rich tasks. By rendering directional forces with high fidelity, the N2D Haptic Glove establishes a basis for next generation of directional wearable haptic interfaces that enable humans to interact with robotic systems as naturally as they do with the physical world. Beyond the studies presented here, the N2D Haptic Glove can be integrated with immersive simulation platforms to create richer training environments [33], [34], applied to medical and industrial teleoperation tasks where precision and feedback are critical [35], and utilized in imitation learning frameworks to provide more informative demonstrations for future robotics research [36]. These directions highlight the broader impact of wearable, multi-directional haptics.

REFERENCES

[1] M. P. S. O. A. J. van der Meijden, "The value of haptic feedback in conventional and robot-assisted minimal invasive surgery and virtual reality training: a current review," *Surgical Endoscopy*, vol. 23, no. 6, pp. 1180–1190, 2009.

[2] C. Cuan, A. Okamura, and M. Khansari, "Leveraging haptic feedback to improve data quality and quantity for deep imitation learning models," *IEEE Transactions on Haptics*, vol. 17, no. 4, pp. 984–991, 2024.

[3] I. Choi, E. Ofek, H. Benko, M. Sinclair, and C. Holz, "Claw: A multifunctional handheld haptic controller for grasping, touching, and triggering in virtual reality," in *Proceedings of the 2018 CHI conference on human factors in computing systems*, pp. 1–13, 2018.

[4] 3D Systems, "3d systems touch haptic device." `https://www.3dsystems.com/haptics-devices/touch`. Accessed: 2025-08-20.

[5] A. Arasan, C. Basdogan, and T. M. Sezgin, "Haptic stylus with inertial and vibro-tactile feedback," in *2013 World Haptics Conference (WHC)*, pp. 425–430, IEEE, 2013.

[6] Y. Tong, H. Liu, and Z. Zhang, "Advancements in humanoid robots: A comprehensive review and future prospects," *IEEE/CAA Journal of Automatica Sinica*, vol. 11, no. 2, pp. 301–328, 2024.

[7] S. Baik, S. Park, and J. Park, "Haptic glove using tendon-driven soft robotic mechanism," *Frontiers in bioengineering and biotechnology*, vol. 8, p. 541105, 2020.

[8] D. Trinitatova and D. Tsetserukou, "Fidtouch: A 3d wearable haptic display for the finger pad," *arXiv preprint arXiv:2507.07661*, 2025.

[9] S. B. Schorr, Z. F. Quek, I. Nisky, W. R. Provancher, and A. M. Okamura, "Tactor-induced skin stretch as a sensory substitution method in teleoperated palpation," *IEEE Transactions on Human-Machine Systems*, vol. 45, no. 6, pp. 714–726, 2015.

[10] L. T. Gwilliam, A. J. Doxon, and W. R. Provancher, "Haptic matching of directional force and skin stretch feedback cues," in *2013 World Haptics Conference (WHC)*, pp. 19–24, IEEE, 2013.

[11] H. Kim, H. Yi, H. Lee, and W. Lee, "Hapcube: A wearable tactile device to provide tangential and normal pseudo-force feedback on a fingertip," in *Proceedings of the 2018 CHI Conference on Human Factors in Computing Systems*, pp. 1–13, 2018.

[12] C. Pacchierotti, D. Prattichizzo, and K. J. Kuchenbecker, "Cutaneous feedback of fingertip deformation and vibration for palpation in robotic surgery," *IEEE Transactions on Biomedical Engineering*, vol. 63, no. 2, pp. 278–287, 2015.

[13] M. Bouzit, G. Burdea, G. Popescu, and R. Boian, "The rutgers master ii-new design force-feedback glove," *IEEE/ASME Transactions on mechatronics*, vol. 7, no. 2, pp. 256–263, 2002.

[14] K. Song, S. H. Kim, S. Jin, S. Kim, S. Lee, J.-S. Kim, J.-M. Park, and Y. Cha, "Pneumatic actuator and flexible piezoelectric sensor for soft virtual reality glove system," *Scientific reports*, vol. 9, no. 1, p. 8988, 2019.

[15] S. Jadhav, V. Kannanda, B. Kang, M. T. Tolley, and J. P. Schulze, "Soft robotic glove for kinesthetic haptic feedback in virtual reality environments," *electronic imaging*, vol. 29, pp. 19–24, 2017.

[16] V. Shen, T. Rae-Grant, J. Mullenbach, C. Harrison, and C. Shultz, "Fluid reality: High-resolution, untethered haptic gloves using electroosmotic pump arrays," in *Proceedings of the 36th Annual ACM Symposium on User Interface Software and Technology*, pp. 1–20, 2023.

[17] S. Patel, Z. Rao, M. Yang, and C. Yu, "Wearable haptic feedback interfaces for augmenting human touch," *Advanced Functional Materials*, p. 2417906, 2025.

[18] R. Hinchet, V. Vechev, H. Shea, and O. Hilliges, "Dextres: Wearable haptic feedback for grasping in vr via a thin form-factor electrostatic brake," in *Proceedings of the 31st Annual ACM Symposium on User Interface Software and Technology*, pp. 901–912, 2018.

[19] J. A. Fishel and G. E. Loeb, "Sensing tactile microvibrations with the biotac—comparison with human sensitivity," in *2012 4th IEEE RAS & EMBS international conference on biomedical robotics and biomechatronics (BioRob)*, pp. 1122–1127, IEEE, 2012.

[20] I. Choi, H. Culbertson, M. R. Miller, A. Olwal, and S. Follmer, "Grabity: A wearable haptic interface for simulating weight and grasping in virtual reality," in *Proceedings of the 30th annual ACM symposium on user interface software and technology*, pp. 119–130, 2017.

[21] Z. F. Quek, S. B. Schorr, I. Nisky, W. R. Provancher, and A. M. Okamura, "Sensory substitution and augmentation using 3-degree-of-freedom skin deformation feedback," *IEEE transactions on haptics*, vol. 8, no. 2, pp. 209–221, 2015.

[22] J. Min, S. Jang, S. Lee, and Y. Cha, "Ultralight soft wearable haptic interface with shear-normal-vibration feedback," *Advanced Intelligent Systems*, p. 2500374, 2025.

[23] Z. Ma and P. Ben-Tzvi, "Design and optimization of a five-finger haptic glove mechanism," *Journal of Mechanisms and Robotics*, vol. 7, no. 4, p. 041008, 2015.

[24] F. Li, J. Chen, G. Ye, S. Dong, Z. Gao, and Y. Zhou, "Soft robotic glove with sensing and force feedback for rehabilitation in virtual reality," *Biomimetics*, vol. 8, no. 1, p. 83, 2023.

[25] H. Zhang, S. Hu, Z. Yuan, and H. Xu, "Doglove: Dexterous manipulation with a low-cost open-source haptic force feedback glove," *arXiv preprint arXiv:2502.07730*, 2025.

[26] X. Gu, Y. Zhang, W. Sun, Y. Bian, D. Zhou, and P. O. Kristensson, "Dexmo: An inexpensive and lightweight mechanical exoskeleton for motion capture and force feedback in vr," in *Proceedings of the 2016 CHI Conference on Human Factors in Computing Systems*, pp. 1991–1995, 2016.

[27] J. Qi, F. Gao, G. Sun, J. C. Yeo, and C. T. Lim, "Hapt-glove—untethered pneumatic glove for multimode haptic feedback in reality–virtuality continuum," *Advanced Science*, vol. 10, no. 25, p. 2301044, 2023.

[28] Y. Ma, T. Xie, P. Zhang, H. Kim, and S. Je, "Airpush: A pneumatic wearable haptic device providing multi-dimensional force feedback on a fingertip," in *Proceedings of the 2024 CHI Conference on Human Factors in Computing Systems*, pp. 1–13, 2024.

[29] A. Lemos, L. Rodrigues da Silva, B. Nagy, P. Barroso, and C. Vimieiro, "Biomechanical hand model: Modeling and simulating the lateral pinch movement," *Experimental Mechanics*, vol. 64, no. 9, pp. 1557–1578, 2024.

[30] K. S. Fok and S. M. Chou, "Development of a finger biomechanical model and its considerations," *Journal of biomechanics*, vol. 43, no. 4, pp. 701–713, 2010.

[31] C. C. Gordon, T. Churchill, C. E. Clauser, B. Bradtmiller, J. T. McConville, I. Tebbetts, and R. A. Walker, "1988 anthropometric survey of u.s. army personnel: Summary statistics (interim report)," Tech. Rep. ADA209600, U.S. Army Natick Research, Development and Engineering Center, Natick, MA, 1989.

[32] S. G. Hart, "Nasa-task load index (nasa-tlx); 20 years later," in *Proceedings of the human factors and ergonomics society annual meeting*, vol. 50, pp. 904–908, Sage publications Sage CA: Los Angeles, CA, 2006.

[33] A. Gani, O. Pickering, C. Ellis, O. Sabri, and P. Pucher, "Impact of haptic feedback on surgical training outcomes: a randomised controlled trial of haptic versus non-haptic immersive virtual reality training," *Annals of Medicine and Surgery*, vol. 83, p. 104734, 2022.

[34] K. Li, S. M. Wagh, N. Sharma, S. Bhadani, W. Chen, C. Liu, and P. Kormushev, "Haptic-act: Bridging human intuition with compliant robotic manipulation via immersive vr," *arXiv preprint arXiv:2409.11925*, 2024.
[35] X. Guo, F. McFall, P. Jiang, J. Liu, N. Lepora, and D. Zhang, "A lightweight and affordable wearable haptic controller for robot-assisted microsurgery," *Sensors*, vol. 24, no. 9, p. 2676, 2024.
[36] K. Li, D. Chappell, and N. Rojas, "Immersive demonstrations are the key to imitation learning," *arXiv preprint arXiv:2301.09157*, 2023.